

Effects of Electron-Electron and Electron-Phonon Interactions in Weakly Disordered Conductors and Heterostructures

A. Sergeev*

Department of ECE, Wayne State University, Detroit, Michigan 48202

M. Yu. Reizer

5614 Naiche Rd. Columbus, Ohio 43213

V. Mitin

Electrical Engineering Department, University at Buffalo, Buffalo, New York 14260

We investigate quantum corrections to the conductivity due to the interference of electron-electron (electron-phonon) scattering and elastic electron scattering from impurities and defects in weakly disordered conductors. The interference corrections are proportional to the Drude conductivity and have various temperature dependencies. The electron-electron interaction results in the $T^2 \ln T$ -correction in a bulk conductors. In a quasi-two-dimensional conductor, $d < L_T = v_F/T$ (d is the thickness, v_F is the Fermi velocity), with 3D electron spectrum ($p_F d > 1$) this correction is linear in temperature and differs from that for 2D electrons (G. Zala et. al., Phys. Rev.B **64**, 214204 (2001)) by a numerical factor. In quasi-one-dimensional conductors with 3D and 2D electron spectra (a wire with radius $r < L_T$ and a strip with width $b < L_T$), temperature-dependent corrections are proportional to $\ln T$. The value and the sign of the corrections depend on the strength of the electron-electron interaction in the triplet channel. The electron interaction via exchange of virtual phonons gives $T^2 \ln T$ -correction. In bulk semiconductors the interaction of electrons with thermal phonons via the screened deformation potential results in T^6 -term and via unscreened deformation potential leads to T^2 -term. For a two-dimensional electron gas in heterostructures, the screened deformation potential gives rise to T^4 -term and the unscreened deformation potential leads to $T^2 \ln T$ -term. At low temperatures the interference of electron-electron and electron-impurity scattering dominates in the temperature-dependent conductivity. At higher temperatures the conductivity is determined by the electron-phonon-impurity interference, which prevails over pure electron-phonon scattering in a wide temperature range, which extends with increasing disorder.

PACS numbers: PACS numbers: 72.10.D

I. INTRODUCTION

Interference of electron scattering mechanisms changes drastically transport properties of disordered conductors. It violates the Mathiessen rule, according to which the contributions to conductivity due to random potential and electron-electron (electron-phonon) interactions are additive. Additional interference terms in conductivity have various temperature dependencies. In the diffusion limit, $T\tau \ll 1$ (τ is the elastic mean free time), Altshuler-Aronov corrections to conductivity have been intensively studied in three-dimensional conductors ($T^{1/2}$ -term) and in two-dimensional structures ($\ln T$ -term).¹

Interference of electron-electron (electron-phonon) scattering and elastic scattering from random potential also modifies significantly the electron transport in the quasi-ballistic limit: $T\tau \gg 1$ for electron-electron interaction and $q_T l \gg 1$ for electron-phonon interaction (q_T is the momentum of a thermal phonon, $l = v_F \tau$ is the electron-mean free path. In weakly disordered conductors the interference corrections are always proportional to the Drude conductivity. Electron-phonon-impurity interference in metals was theoretically studied in our paper.² In the quasi-ballistic limit, $T > u/l$ (u is the

sound velocity), the interference correction to conductivity is quadratic in the electron temperature,

$$\frac{\delta_{eph}\sigma}{\sigma_3} = \left[1 - \frac{\pi^2}{16} - 2 \left(\frac{u_l}{u_t} \right)^3 \right] \frac{2\pi^2 \beta_l T^2}{3\epsilon_F p_F u_l}, \quad (1.1)$$

where $\sigma_n = e^2 v_F^2 \tau \nu_n / n$ is the Drude conductivity in corresponding dimensionality n , ϵ_F and p_F are the Fermi energy and momentum, u_l and u_t are the longitudinal and transverse sound velocities, β_l is the constant of the electron-phonon interaction (see Sec. IV), and ν_n is the electron density of states. It is interesting that the longitudinal phonons give rise to a positive correction to conductivity, while transverse phonons result in a negative correction, which dominates in the temperature-dependent conductivity due to stronger coupling of transverse phonons. This T^2 -term proportional to the Drude conductivity have been observed in a wide temperature range, from 20K up to 200K, in Nb, Al, Be³, NbC⁴, NbN⁵, and W⁶ films.

Electron-phonon interaction via the piezoelectric potential in weakly disordered heterostructures was considered in the paper.⁷ It has been found that at low temperatures, $T \leq 0.5$ K, where the piezoelectric potential is

strongly screened, the interference correction is given by

$$\frac{\delta_{pz}\sigma}{\sigma_2} \simeq -\frac{(eh_{14})^2}{4\rho u^3} \frac{T^2}{(\kappa_2 v_F)^2}, \quad (1.2)$$

where h_{14} is piezoelectric constant, κ_2^{-1} is the screening length, and ρ is the density.

Investigation of the electron-electron interaction in weakly disordered 2D electron systems has a long story.^{7,8,9,10,11} After series of improvements, all exchange (Fock) and direct (Hartree) processes have been taken into account in the frame of the Landau Fermi-liquid theory in the paper.¹¹ In the quasiballistic limit, $T\tau > 1$, the correction to conductivity is

$$\frac{\delta_{ee}\sigma}{\sigma_2} = \left(1 + \frac{3F_0^\sigma}{1 + F_0^\sigma}\right) \frac{T}{\epsilon_F}, \quad (1.3)$$

where F_0^σ is the Fermi-liquid parameter describing interaction in the triplet channel. Results of recent measurements in GaAs/GaAsAl heterostructures^{12,13} and Si MOSFETs^{14,15} have shown good agreement with the theory¹¹ at subkelvin (GaAs/GaAlAs) and helium (Si) temperatures. At higher temperatures, the electron-phonon interaction dominates over electron-electron scattering. While electron-phonon processes are also very sensitive to disorder, the deformation electron-phonon interaction in quasi-ballistic regime has not been studied to date.

We would like to stress, that the interference corrections due to the electron-phonon or electron-electron interactions always originate from the *elastic part* of the corresponding collision integral.^{1,2,11} Therefore, the interference corrections depend on the electron temperature only. Early theoretical papers on the electron-phonon-impurity interference considered inelastic scattering from vibrating impurities and extracted the T^2 -correction to conductivity from the inelastic part of the collision integral.¹⁶ However, as it is shown in our previous work,² such terms cancel out and this is a reason why the T^2 -term is independent on the phonon temperature.

In the current paper we continue studying weakly disordered conductors. We calculate various interference corrections not considered before. In Sec. II we start with the basic equations describing interference phenomena in the electron transport. In Sec. III we calculate the electron-electron corrections to the conductivity in various dimensions with respect to the effective interaction. The cross-over to the lower dimensionality occurs when one of the conductor dimensions becomes smaller than q_c^{-1} , where q_c is the characteristic value of the transferred electron momentum. For the electron-electron interaction in weakly disordered conductors, q_c^{-1} is of the order of $L_T = v_F/T$. At sub-Kelvin and helium temperatures, $L_T \sim 1 - 10\mu\text{m}$, and the transition to the quasi-two-dimensional case happens in relatively thick films with the three-dimensional electron spectra and electron screening. The transition to the quasi-one-dimensional case occurs in wires of radius $r \sim L_T$ and in 2D conducting channels of width $b \sim L_T$. We will show that

the interference corrections to the conductivity is mainly determined by the sample dimensionality with respect to the effective interaction. Dimensionality of the electron spectrum just slightly changes numerical coefficients of the interference corrections.

In Sec. IV we calculate corrections to conductivity due to the electron-phonon interaction. We study interaction of electrons by means of virtual phonons and interaction of electrons with thermal phonons in bulk semiconductors and low-dimensional structures. Considering the electron-phonon scattering, we will assume good matching between the conducting and buffer layers and limit our consideration to three-dimensional phonons. In Conclusions, we summarize our main results, compare different terms, and discuss experimental identification of interference contributions to conductivity.

II. BASIC EQUATIONS

Effects of interference between scattering mechanisms on the electron transport can be studied by the linear response method as well as by the quantum transport equation. Both methods are based on the digrammatic technique. The linear response method requires many diagrams to be considered, while the transport equation deals only with the electron self-energy diagrams but includes specific terms in the form of Poisson brackets.^{2,7}

In this paper we investigate the interference electron processes, which are characterized by the momentum transfer much smaller than the Fermi momentum. These processes can be described in the frame of the Landau Fermi-liquid theory. The corresponding self-energy diagrams for weakly disordered systems are shown in Fig. 1 and the diagrams of the linear response method are presented in Fig. 2. Results of the papers,^{2,7,11} which are briefly reproduced in Appendix, show that in the quasiballistic limit the correction to conductivity may be presented as

$$\frac{\delta_{int}\sigma^{(k)}}{\sigma_n} = 2 \int \frac{d\omega}{2\pi} \frac{d^k q}{(2\pi)^k} \frac{f(\omega)}{\omega^2} \Im \Upsilon_n^{(k)}(q, \omega), \quad (2.1)$$

where k is the dimensionality of the conductor with respect to the interaction and n is used for the dimensionality of the electron spectrum. As we discussed in Introduction, the dimensionality with respect to the effective electron-electron interaction is determined by the characteristic length $L_T = v_F/T$.

The function $f(\omega)$ is given by

$$f(\omega) = \frac{\partial}{\partial \omega} \left[\omega \coth \left(\frac{\omega}{2T} \right) \right]. \quad (2.2)$$

The function $\Upsilon(q, \omega)$ is given by

$$\Upsilon_n^{(k)}(q, \omega) = (\omega\tau)^2 V_n^R(\mathbf{q}, \omega) \Phi_n^{(k)}(q, \omega), \quad (2.3)$$

where $V_n^R(\mathbf{q}, \omega)$ is the retarded propagator describing electron-electron or electron-phonon interaction, and

$\Phi(q, \omega)$ is given by

$$\begin{aligned} \Phi_n^{(k)}(q, \omega) = & -\frac{n}{v_F^2 \tau^2} \left[\left\langle \left\langle \frac{\gamma^2 (\mathbf{v}_F \mathbf{e})^2}{(\mathbf{q} \mathbf{v}_F - \omega - i0)^2} \right\rangle \right\rangle_{\mathbf{v}, \mathbf{q}} \right. \\ & - \left\langle \left\langle \frac{\gamma (\mathbf{v}_F \mathbf{e})^2}{\mathbf{q} \mathbf{v}_F - \omega - i/\tau} \right\rangle \right\rangle_{\mathbf{v}, \mathbf{q}} \cdot \left\langle \left\langle \frac{\gamma}{\mathbf{q} \mathbf{v}_F - \omega - i0} \right\rangle \right\rangle_{\mathbf{v}} \\ & + \left. \left\langle \left\langle \frac{\gamma \mathbf{v}_F \mathbf{e}}{\mathbf{q} \mathbf{v}_F - \omega - i0} \right\rangle \right\rangle_{\mathbf{v}, \mathbf{q}}^2 \right]. \end{aligned} \quad (2.4)$$

In Eq. 2.4, γ is the vertex of the electron-electron or electron-phonons interaction, $\mathbf{e} = \mathbf{E}/E$ is the unit vector in the direction of the electric field, and $\langle \rangle_{\mathbf{v}(\mathbf{q})}$ stands for the averaging over the directions of \mathbf{v}_F and \mathbf{q} .

For isotropic conductors ($n=k$), the averaging over the \mathbf{p} and \mathbf{q} directions is reduced to the averaging over the angle ϕ , the angle between \mathbf{p} and \mathbf{q} . In this case, Eq. 2.4 can be simplified,

$$\begin{aligned} \tau^2 \Phi_n^{(n)}(q, \omega) = & - \left\langle \left\langle \frac{\gamma^2}{(\mathbf{q} \mathbf{v}_F - \omega - i0)^2} \right\rangle \right\rangle_{\phi} \\ & + \left\langle \left\langle \frac{\gamma}{\mathbf{q} \mathbf{v}_F - \omega - i0} \right\rangle \right\rangle_{\phi}^2 - \left\langle \left\langle \frac{\mathbf{q} \mathbf{v}_F}{qv_F} \frac{\gamma}{\mathbf{q} \mathbf{v}_F - \omega - i0} \right\rangle \right\rangle_{\phi}^2 \end{aligned} \quad (2.5)$$

Note, that in this form Eq. 2.5 is applicable to any dimensionality of the electron system,

$$\langle \psi(\mathbf{q} \mathbf{v}_F) \rangle_{\phi} = \begin{cases} \int_{-1}^1 \psi(qv_F x) \frac{dx}{2}, & 3D; \\ \int_0^{2\pi} \psi(qv_F \cos \phi) \frac{d\phi}{2\pi} & 2D; \\ \frac{1}{2} \sum_{x=\pm 1} \psi(qv_F x) & 1D, \end{cases} \quad (2.6)$$

where $x = \cos(\phi)$.

In the next sections we use equation derived in this section to calculate the quantum corrections to conductivity due to electron-electron and electron-phonon interactions in weakly disordered conductors of various dimensionality with respect to the electron spectrum (n) and with respect to the interaction (k).

III. ELECTRON-ELECTRON INTERACTION

As we discussed in the introduction, the effective electron-electron interaction in weakly disordered conductors is characterized by the momentum transfer of the order of T/v_F , which is much smaller than the Fermi momentum (see also calculations below). Therefore, the electron transport can be described in the frame of the Landau Fermi-liquid theory.¹¹ In the singlet channel the bare interaction is given the sum of the Coulomb poten-

tial,

$$V_0(q) = \begin{cases} \frac{4\pi e^2}{q^2}, & 3D; \\ \frac{2\pi e^2}{|q|}, & 2D; \\ e^2 \ln \frac{1}{q^2 \tau^2}, & 1D, \end{cases} \quad (3.1)$$

and the Fermi-liquid interaction,

$$V_F \approx -F_0^p / \nu_n. \quad (3.2)$$

The screened interaction in the random phase approximation, which is justified for small momentum transfers, is given by

$$V_n^{R(A)}(q, \omega) = \frac{\nu_n V_0(q) - F_0^p}{\nu_n - [\nu_n V_0(q) - F_0^p] P_n^{R(A)}(q, \omega)}, \quad (3.3)$$

where $P^{R(A)}(q, \omega)$ is the polarization operator.

In the absence of the magnetic field and spin-orbit scattering the screened propagator in the triplet-channel may be taken in the form¹¹

$$V_n^{R(A)}(\mathbf{q}, \omega) = -\frac{3F_0^\sigma}{\nu_n - F_0^\sigma P_n^{R(A)}(\mathbf{q}, \omega)}, \quad (3.4)$$

where F_0^σ is the Fermi-liquid constant. The above equation assumes that the Fermi-liquid coupling is independent on electron momenta. Restrictions of this approximation were discussed in the paper¹¹.

In the Subsecs. A and B we calculate the conductivity corrections in the singlet channel, the triplet-channel corrections will be studied in Subsec. C.

A. Systems with three-dimensional spectrum

First we consider a conductor with three-dimensional electron spectrum. For $1/\tau \ll \omega \lesssim qv_F \ll \epsilon_F$, the polarization operator is given by

$$P_3^R(q, \omega) = -\nu_3 \left[1 - \frac{\omega}{qv_F} \operatorname{arctanh} \left(\frac{qv_F}{\omega + i0} \right) \right], \quad (3.5)$$

where the branch of $\operatorname{arctanh}(y)$ is chosen as

$$\operatorname{arctanh}(y) = -\frac{\pi i}{2} + \frac{1}{2} \ln \frac{y+1}{y-1}, \quad y > 1. \quad (3.6)$$

Thus, the screened Coulomb potential may be presented as

$$V_3^R(q, \omega) = \frac{\frac{1}{\nu_3} \left(1 - F_0^p \frac{q^2}{\kappa_3^2} \right)}{\frac{q^2}{\kappa_3^2} + \left(1 - F_0^p \frac{q^2}{\kappa_3^2} \right) \left[1 - \frac{\operatorname{arctanh}(qv_F/\omega)}{qv_F/\omega} \right]} \quad (3.7)$$

where $\kappa_3^2 = 4\pi e^2 \nu_3$, and $\nu_3 = mp_F/\pi^2$. In the limit of strong screening, $\kappa_3 \gg q$, the screened potential is independent on the form of the bare potential (the unitary limit).

Taking into account that for the electron-electron interaction $\gamma = 1$ and calculating integrals in Eq. 2.5, we find

$$\Phi_3^{(3)}(q, \omega) = \frac{1}{\tau^2} \left[\frac{1}{(qv_F)^2 - (\omega)^2} + \left(\frac{\text{arctanh}(qv_F/\omega)}{qv_F} \right)^2 - \frac{1}{(qv_F)^2} \left(1 - \frac{\text{arctanh}(qv_F/\omega)}{qv_F/\omega} \right)^2 \right]. \quad (3.8)$$

Substituting $\Phi(q, \omega)$ and $V^R(q, \omega)$ into Eq. 2.1, we get the correction to the conductivity in the singlet channel. For simplicity we present further results in the limit $\kappa_3 \gg q$. Then,

$$\frac{\delta_{ee}^s \sigma}{\sigma_3} = 2 \int \frac{d\omega}{2\pi} \frac{f(\omega)}{\omega^2} \int_{|\omega|/v_F}^{2p_F} \frac{q^2 dq}{2\pi^2} \Im \Upsilon_3^{(3)} \left(\frac{qv}{\omega} \right), \quad (3.9)$$

where

$$\begin{aligned} \Upsilon_3^{(3)}(y) &= \frac{1}{\nu_3} \frac{1}{1 - \text{arctanh}(y)/y} \\ &\times \left[\frac{1}{y^2 - 1} + \left(\frac{\text{arctanh } y}{y} \right)^2 - \left(\frac{1}{y} - \frac{\text{arctanh } y}{y^2} \right)^2 \right]. \end{aligned} \quad (3.10)$$

Note, the low limit in the integral in Eq. 3.9 is chosen taking into account that the imaginary part of $\Upsilon(qv/\omega)$ exists only at $y = qv_F/\omega \geq 1$.

The function $\Upsilon_3(qv_F/\omega)$ has the following asymptotes

$$\Im \Upsilon_3^{(3)}(y) = \frac{1}{\nu_3} \begin{cases} \left(\frac{\pi^3}{8} - 2\pi \right) \frac{1}{y^3}, & y \rightarrow \infty, \\ -\frac{\pi}{(\ln(y-1))^2} \frac{1}{(y-1)}, & y \rightarrow 1. \end{cases} \quad (3.11)$$

Therefore, with logarithmic accuracy we get

$$\frac{v_F^3 \nu_3}{\omega^3} \int_{|\omega|/v_F}^{2p_F} dq q^2 \Im \Upsilon_3^{(3)} \left(\frac{qv_F}{\omega} \right) = \left(\frac{\pi^3}{8} - 2\pi \right) \ln \frac{4\epsilon_F}{|\omega|}. \quad (3.12)$$

As seen from Eqs. 3.12, the integral over q covers the interval from $\omega/v_F \sim T/v_F$ to $2p_F$, but the temperature dependence arises only from the low limit, $q = T/v_F$. Therefore, the approximation, $q \ll p_F$, which we made for the polarization operator (Eq. 3.5) is justified by the logarithmic accuracy of the integral in Eq. 3.12.

Finally, taking into account that

$$\int d\omega \omega f(\omega) \ln \frac{\epsilon_F}{|\omega|} = -\frac{2\pi^2 T^2}{3} \ln \frac{4\epsilon_F}{T}, \quad (3.13)$$

we find

$$\frac{\delta_{ee}^s \sigma^{(3)}}{\sigma_3} = C_3 \left(\frac{T}{\epsilon_F} \right)^2 \ln \frac{4\epsilon_F}{T}, \quad (3.14)$$

$$C_3 = \frac{\pi^2}{6} \left(1 - \frac{\pi^2}{16} \right). \quad (3.15)$$

We would like to remind that this result has been obtained in the limit of strong screening, $\kappa_3 \gg 2p_F$, where the screened potential does not depend on the bare potential. Our calculations show that in the general case, $\kappa_3 \sim 2p_F$, the leading term, $T^2 \ln T$, is also given by Eq. 3.14, while additional terms are proportional to T^2 .

Next we consider a quasi-two-dimensional conductor with 3D electron spectrum. For a film or conducting layer of finite thickness d , integration over the transverse component of the wavevector q in Eq. 2.1 is replaced by summation over eigenstates in the film. As seen from Eqs. 3.12 and 3.13, the characteristic value of ω is of the order of T and the characteristic values of the momentum q is ω/v_F . Therefore, a transition to quasi-two-dimensional case occurs, if the thickness of a conducting layer, d , is of the order of the characteristic length $L_T = v_F/T$. For a quasi-two-dimensional conductor, $d \ll L_T$, the electron transitions with $q_\perp = 0$ should be retained,

$$\frac{d^3 q}{(2\pi)^3} \rightarrow \frac{1}{d} \frac{d^2 q}{(2\pi)^2} \delta_{q_\perp, 0}. \quad (3.16)$$

Averaging Eq. 2.4 over the directions of vectors \mathbf{q} and \mathbf{v}_F , one should take into account that vectors \mathbf{q} and \mathbf{e} lie in the plane of the conductor, while the vector \mathbf{v}_F has an arbitrary direction. In this geometry we get

$$\begin{aligned} \Phi_3^{(2)}(q, \omega) &= -\frac{3}{\tau^2} \left[\frac{1}{4} \left\langle \frac{(1+x^2)}{(qv_F x - \omega - i0)^2} \right\rangle_\phi \right. \\ &- \frac{1}{4} \left\langle \frac{(1+x^2)}{qv_F x - \omega - i/\tau} \right\rangle_\phi \cdot \left\langle \frac{1}{qv_F x - \omega - i0} \right\rangle_\phi \\ &\left. + \frac{1}{2} \left\langle \frac{x}{qv_F x - \omega - i0} \right\rangle_\phi^2 \right], \end{aligned} \quad (3.17)$$

where $x = \cos \phi$ and the averaging over the angle ϕ is given by Eq. 2.6.

Calculating $\Phi_3^{(2)}(q, \omega)$, in the limit of strong screening we get the function $\Upsilon(qv_F/\omega)$ defined by Eq. 2.3,

$$\begin{aligned} \nu_3 \Upsilon_3^{(2)}(y) &= \frac{3}{4y^2} \left(1 - \frac{\text{arctanh } y}{y} \right)^{-1} \\ &\times \left[\frac{4-2y^2}{y^2-1} + \frac{5\text{arctanh } y}{y} + (y^2-1) \left(\frac{\text{arctanh } y}{y} \right)^2 \right]. \end{aligned} \quad (3.18)$$

Thus, the correction to the conductivity (Eq. 2.1) is given by

$$\frac{\delta_{ee}^s \sigma^{(2)}}{\sigma_3} = -\frac{1}{\pi^2 d v_F^2 \nu_3} C_2 \int_0^{\epsilon_F} d\omega f(\omega), \quad (3.19)$$

where

$$C_2 = -\int_1^\infty dy y \nu_3 \Im \Upsilon_3^{(2)}(y) \approx 5.3 \quad (3.20)$$

Here the integral over q can be extended to infinity, because only processes with small momentum transfer,

$q \sim \omega/v_F$, are important. Taking into account that

$$\int_0^{\epsilon_F} d\omega f(\omega) = -2T + \epsilon_F \coth\left(\frac{\epsilon_F}{2T}\right), \quad (3.21)$$

we see that the temperature dependent correction to the conductivity is determined by the first term in Eq. 3.21. From Eq. 3.19 we find

$$\frac{\delta_{ee}^s \sigma^{(2)}}{\sigma_3} = \frac{C_2}{p_F d} \frac{T}{\epsilon_F}. \quad (3.22)$$

In Eq. 3.22 we omit additional term proportional to $(T/\epsilon_F)^2 \ln(p_F d)$. It originates from the interval $1/d \ll q \leq 2p_F$ and it is small compared with the linear term.

Now we consider quasi-one-dimensional conductors, such as wires with radius r , which is much smaller than L_T . In this case the integration over the transfer momentum in Eq. 2.1 is replaced by

$$\frac{d^3 q}{(2\pi)^3} \rightarrow \frac{1}{\pi r^2} \frac{dq}{2\pi} \delta_{q_\perp, 0}. \quad (3.23)$$

In the quasi-one-dimensional case the vectors \mathbf{q} and \mathbf{e} are parallel. Averaging Eq. 2.4 over the angles of \mathbf{q} we get

$$\Phi_3^{(1)}(q, \omega) = -\frac{3}{\tau^2} \left[\left\langle \frac{x^2}{(qv_F x - \omega - i0)^2} \right\rangle_\phi - \left\langle \frac{x^2}{qv_F x - \omega - i/\tau} \right\rangle_\phi \cdot \left\langle \frac{1}{qv_F x - \omega - i0} \right\rangle_\phi \right]. \quad (3.24)$$

In the limit of strong screening, the function $\Upsilon(qv_F/\omega)$ (Eq. 2.3), is given by

$$\nu_3 \Upsilon_3^{(1)}(y) = \frac{3}{y^2} \left(1 - \frac{\operatorname{arctanh} y}{y} \right)^{-1} \times \left[\frac{2 - 2y^2}{y^2 - 1} + \frac{\operatorname{arctanh} y}{y} + \left(\frac{\operatorname{arctanh} y}{y} \right)^2 \right]. \quad (3.25)$$

Then, the correction to the conductivity (Eq. 2.1) is

$$\frac{\delta_{ee}^s \sigma^{(1)}}{\sigma_3} = -\frac{1}{\pi^3 r^2 v_F \nu_3} C_1 \int_0^{\epsilon_F} d\omega \frac{f(\omega)}{\omega}, \quad (3.26)$$

where

$$C_1 = -\int_1^\infty dy y \nu_3 \Im \Upsilon_3^{(1)}(y) \approx 4.3 \quad (3.27)$$

Taking into account that

$$\int_0^{\epsilon_F} d\omega \frac{f(\omega)}{\omega} = \ln\left(\frac{\epsilon_F}{2T}\right), \quad (3.28)$$

finally we get

$$\frac{\delta_{ee}^s \sigma^{(1)}}{\sigma_3} = \frac{C_1}{\pi (r p_F)^2} \ln\left(\frac{2T}{\epsilon_F}\right). \quad (3.29)$$

B. Two-dimensional electron spectrum

Next we calculate the interference correction in conductors with two-dimensional electron spectra. For 2D electron gas the polarization operator in the quasi-ballistic limit is

$$P_2^R(q, \omega) = -\nu_2 \left(1 - \frac{\omega}{\sqrt{(\omega + i0)^2 - (qv_F)^2}} \right), \quad (3.30)$$

where $\nu_2 = m/\pi$. Using Eq. 2.5, in the limit of strong screening, $V^R(q, \omega) = -1/P_2^R(q, \omega)$, we get¹¹

$$\nu_2 \Upsilon_2^{(2)}(y) = \frac{1}{1 - (y - i0)^2} + \frac{1}{y^2 \sqrt{1 - (y - i0)^2}}, \quad (3.31)$$

and the corresponding correction to the conductivity (Eq. 2.1) is given by

$$\frac{\delta_{ee}^s \sigma^{(2)}}{\sigma_2} = -\frac{1}{\pi v_F^2 \nu_2} \int_0^{\epsilon_F} d\omega f(\omega). \quad (3.32)$$

The integral over ω in Eq. 3.32 is exactly the same as in the case of quasi-two-dimensional conductor (Eq. 3.21). Finally, we get the correction to conductivity given by Eq. 1.3. As seen, in the quasi-ballistic limit the polarization operator (Eqs. 3.5 and 3.30) and the function $F(y)$ (Eqs. 3.18 and 3.31) has different forms for quasi-two-dimensional and two-dimensional conductors. Therefore, the final results (Eqs. 1.3 and 3.22) differ by a numerical factor.

Next we consider conductivity in the quasi-one-dimensional conductor, such as a narrow channel with width $b < L_T$. Taking into account that in the quasi-one-dimensional case the vectors \mathbf{q} and \mathbf{E} are parallel and averaging Eq. 2.4 over the angles of \mathbf{q} , we get

$$\Phi_2^{(1)}(q, \omega) = -\frac{2}{\tau^2} \left[\left\langle \frac{(\cos \phi)^2}{(qv_F \cos \phi - \omega - i0)^2} \right\rangle_\phi - \left\langle \frac{(\cos \phi)^2}{qv_F \cos \phi - \omega - i/\tau} \right\rangle_\phi \cdot \left\langle \frac{1}{qv_F \cos \phi - \omega - i0} \right\rangle_\phi \right]. \quad (3.33)$$

After averaging over the angle ϕ , we find

$$\Phi_2^{(1)}(q, \omega) = \frac{2}{\tau^2} \frac{1}{(\omega + i0)^2 - (qv)^2} \times \left[1 - \frac{\omega}{\sqrt{(\omega + i0)^2 - (qv)^2}} \right]. \quad (3.34)$$

Therefore, in the unitary limit, the function $\Upsilon(qv_F/\omega)$ (Eq. 2.3), is given by

$$\nu_2 \Upsilon_2^{(1)}(y) = \frac{2}{1 - (y - i0)^2}. \quad (3.35)$$

Calculating the correction to the conductivity in the singlet channel,

$$\frac{\delta_{ee}^s \sigma^{(1)}}{\sigma_2} = \frac{1}{\pi^2 \nu_2 v_F b} \int_0^{\epsilon_F} d\omega \frac{f(\omega)}{\omega} \int_0^\infty dy \Im \Upsilon_2^{(1)}(y), \quad (3.36)$$

(3.38)

TABLE I: Corrections to the conductivity $\delta_{ee}^s \sigma^k / \sigma_n$ due to electron-electron interaction in the singlet channel.

n / k ^a	k=3	k=2	k=1
n=3	$\frac{C_3 T^2}{\epsilon_F^2} \ln \frac{4\epsilon_F}{T}$	$\frac{C_2}{p_F d} \frac{T}{\epsilon_F}$	$\frac{C_1}{\pi (r p_F)^2} \ln \frac{2T}{\epsilon_F}$
n=2	-	$\frac{T}{\epsilon_F}$	$\frac{1}{p_F b} \ln \frac{2T}{\epsilon_F}$

^a n is the dimensionality of a conductor with respect to electron spectrum, k is the dimensionality with respect to the interaction (crossover to low dimensionality occurs at the characteristic length $L_T = v_F/T$); σ_n is the Drude conductivity; d is the thickness of a quasi-two-dimensional conductor, r is the radius of a quasi-one-dimensional conductor, b is the width of a conductor curved from 2D-layer; C_1, C_2 , and C_3 are numerical constants defined by Eqs. 3.27, 3.20, and 3.14.

we get

$$\frac{\delta_{ee}^s \sigma^{(1)}}{\sigma_2} = \frac{1}{p_F b} \ln \left(\frac{2T}{\epsilon_F} \right). \quad (3.37)$$

Thus, in quasi-one-dimensional conductors with 3D electron spectra (Eq. 3.29) and 2D spectra (Eq. 3.37) the corrections have the logarithmic temperature dependence.

The main results of Subsecs. A and B are summarized in Tab. 1. In these subsections we have considered the singlet-channel interaction in the limit of strong screening (the unitary limit), which gives the upper bound for the strength of the interelectron interaction. As it follows from calculations above, the characteristic value of the electron momentum transferred is of the order of T/v_F . Thus, the leading corrections to conductivity are accumulated at large distances, $L_T \simeq \hbar v_F / k_B T$, where the electron-electron interaction is strongly screened. In the unitary limit the interaction has an universal form, which is independent of the original interaction and its renormalization by the Fermi liquid parameters.

C. Triplet channel interaction

Conductivity corrections in the triplet channel are calculated in the same way as the singlet-channel corrections. Substituting the triplet-channel propagator (Eq. 3.4) and the function $\Phi_3^{(3)}$ (Eq. 3.8 in Eq. 2.3) into Eq. 2.3, we find the function $\Upsilon(y)$ for a bulk conductor,

$$\begin{aligned} \Upsilon_3^{(3)}(y) &= \frac{1}{\nu_3} \frac{3F_0^\sigma}{1 + F_0^\sigma \left(1 - \operatorname{arctanh}(y)/y \right)} \\ &\times \left[\frac{1}{y^2 - 1} + \left(\frac{\operatorname{arctanh} y}{y} \right)^2 - \left(\frac{1}{y} - \frac{\operatorname{arctanh} y}{y^2} \right)^2 \right]. \end{aligned}$$

Finally, integrating Eq. 3.9, with logarithmic accuracy we get

$$\begin{aligned} \frac{\delta_{ee}^t \sigma^{(3)}}{\sigma_3} &= \frac{3F_0^\sigma}{1 + F_0^\sigma} \left(1 - \frac{\pi^2}{16} \frac{F_0^\sigma}{1 + F_0^\sigma} \right) \\ &\times \frac{\pi^2}{6} \left(\frac{T}{\epsilon_F} \right)^2 \ln \frac{4\epsilon_F}{T}. \end{aligned} \quad (3.39)$$

Results for the quasi-two and quasi-one-dimensional conductors with 3D spectrum cannot be presented in analytical form and will not be considered here.

In the case of the quasi-one-dimensional conductor carved from the two-dimensional structure (see Subsec. B), the function $\Upsilon(y)$ is given by

$$\begin{aligned} \Upsilon_2^{(1)}(y) &= -\frac{1}{\nu_2} \frac{3F_0^\sigma}{1 + F_0^\sigma} \frac{2}{1 - (y - i0)^2} \\ &\times \left(1 - \frac{1}{(1 + F_0^\sigma) \sqrt{1 - y^2 - F_0^\sigma}} \right). \end{aligned} \quad (3.40)$$

Finally, integrating Eq. 3.36, we get

$$\frac{\delta_{ee}^t \sigma^{(1)}}{\sigma_2} = \frac{3 \left(F_0^\sigma + \pi G(F_0^\sigma) \right)}{1 + F_0^\sigma} \frac{1}{p_F b} \ln \left(\frac{2T}{\epsilon_F} \right), \quad (3.41)$$

where

$$\begin{aligned} G(F_0^\sigma) &= -1 - \frac{2}{\pi} \frac{|1 + F_0^\sigma|}{\sqrt{|1 + 2F_0^\sigma|}} \\ &\times \begin{cases} \operatorname{arctanh} \frac{\sqrt{-1 - 2F_0^\sigma}}{F_0^\sigma}, & F_0^\sigma < -\frac{1}{2}, \\ \operatorname{arctan} \frac{\sqrt{1 + 2F_0^\sigma}}{F_0^\sigma}, & -\frac{1}{2} < F_0^\sigma < 0, \\ \operatorname{arctan} \frac{\sqrt{1 + 2F_0^\sigma}}{F_0^\sigma} - \pi, & F_0^\sigma > 0. \end{cases} \end{aligned} \quad (3.42)$$

Thus, the temperature dependence of the conductivity corrections in the triplet channel (Eqs. 3.39 and 3.41) is the same as in the singlet channel, but the value and sign depend on the parameter F_0^σ .

IV. ELECTRON-PHONON INTERACTION

To apply Eqs. 2.1 and 2.5 to the electron-phonon interaction one should specify the phonon propagator and electron phonon vertex. The retarded phonon Green function is given by

$$D^R(\mathbf{q}, \omega) = (\omega - \omega_{\mathbf{q}} + i0)^{-1} - (\omega + \omega_{\mathbf{q}} + i0)^{-1}. \quad (4.1)$$

The unscreened vertex of the electron-phonon scattering due to the deformation potential is

$$\gamma = \frac{D\mathbf{q} \cdot \mathbf{e}_n}{(2\rho\omega_{\mathbf{q}})^{1/2}}, \quad (4.2)$$

where \mathbf{e}_n is the phonon polarization vector.

In the isotropic model, for longitudinal phonons the deformation potential is described by two constants D_0 and G ,¹⁷

$$D = D_0 - 3G(\cos\theta)^2. \quad (4.3)$$

Screening of the bare electron-phonon vertex presented in Fig. 3 leads to

$$\gamma_{sc} = \frac{q}{(2\rho\omega_q)^{1/2}} \left[\frac{D_0}{1 - V_0(q)P^R(q, \omega)} - 3G \left((\cos\theta)^2 + \frac{V_0(q)P_2^R(q, \omega)}{1 - V_0(q)P(q, \omega)} \right) \right], \quad (4.4)$$

where $P(q, \omega)$ is given by Eq. 3.5, and $P_2(q, \omega)$ is the electron polarization operator with the vertex $(\cos\theta)^2$.

In a semiconductor, the deformation potential constant D_0 is much larger than the constant G , which has strong concentration dependence (see below). For this reason, the first term in the square brackets in Eq. 4.4 is only taken into account. For thermal phonons qv_F is much larger than ω , and, therefore, the dynamic part of $P(q, \omega)$ proportional to ω may be neglected. Therefore, in a semiconductor interaction between electrons and real phonons is described by the vertex

$$\gamma_{sem} = \frac{q}{(2\rho\omega_q)^{1/2}} \frac{D_0}{1 + \kappa_3^2/q^2}. \quad (4.5)$$

In a metal two constants of the deformation potential D_0 and G are of the same order. However, due to the strong screening ($V_0(q)P^R(q, \omega) \gg 1$), the term with the constant D_0 in Eq. 4.4 becomes negligible¹⁷. Thus, for a metal we get

$$\gamma_{met} = \frac{Gq}{(2\rho\omega_q)^{1/2}} \left[\left(1 - \frac{\omega\tau}{ql} \operatorname{arctanh}\left(\frac{ql}{\omega\tau}\right) \right)^{-1} + 3 \left(\frac{\omega}{qv} \right)^2 - 3(\cos\theta)^2 \right], \quad (4.6)$$

In the static limit, $ql \gg \omega\tau$, which is applicable to the thermal phonons, the last equation reduces to

$$\gamma_{met} = [1 - (3\cos\theta)^2] \frac{Gq}{(2\rho\omega_q)^{1/2}}, \quad (4.7)$$

where $G = (2/3)\epsilon_F^{2,17}$.

Vertices obtained in this section will be used to calculate interference correction to conductivity due to virtual phonons (Sec. V) and thermal phonons (Sec. VI).

A. Virtual phonons

Besides the Coulomb potential, the electron-electron interaction may be realized via intermediate electron-ion interaction, i.e. via virtual phonons. If $\omega_q = qu \gg \omega \sim$

T , according to Eq. 4.1, the phonon propagator D^R is real and equal to $-2/\omega_q$. Then, from Eq. 2.1 we get

$$\frac{\delta_{e-v.ph}\sigma}{\sigma_3} = -4\tau^2 \int \frac{d\omega}{2\pi} \frac{q^2 dq}{2\pi^2} f(\omega) \omega_q^{-1} \Im\Phi(q, \omega). \quad (4.8)$$

We start with the electron-phonon interaction due to the deformation potential (D_0) in a bulk semiconductor. In this case the square of the electron-phonon vertex does not have an imaginary part, and the function $\Im\Phi(q, \omega)$ is given by Eq. 3.8. Integrating Eq. 4.8 over q , one should take into account the characteristic interval $T/u < q < 2p_F$. Therefore, with logarithmic accuracy we get

$$\frac{\delta_{e-v.ph}^{sem}\sigma}{\sigma_3} = -\frac{2D_0^2 T^2}{3\rho v_F^3 u^2} \ln\left(\frac{p_F u}{T}\right). \quad (4.9)$$

In metals the deformation potential is effectively screened, and in $\Im\Phi(q, \omega)$ one should take into account the imaginary part of the electron-phonon vertex (Eq. 4.6). Calculating the integrals in Eq. 2.5 with the vertex γ_{met} (Eq. 4.6) we find

$$\Im\Phi(q, \omega) = -2\pi \left(\frac{\pi^2}{8} - 1 \right) \frac{\omega\tau}{ql}. \quad (4.10)$$

Substituting this result into Eq. 4.8 we get

$$\frac{\delta_{e-v.ph}^{met}\sigma}{\sigma_3} = \frac{8}{27} \left(\frac{\pi^2}{8} - 1 \right) \frac{\epsilon_F^2 T^2}{\rho v_F^3 u^2} \ln\left(\frac{p_F u}{T}\right). \quad (4.11)$$

Note, that large electron momentum is transferred via exchange of virtual phonons. According to Sec. III, such processes are important only in conductors with 3D electron spectrum. In 2D structures, the electron-electron correction is associated with processes of small momentum transfer, therefore, the contribution of virtual phonons is absent.

B. Thermal Phonons

For thermal phonons, the imaginary part of the phonon propagator (Eq. 4.1) is only important,

$$\Im D^R(q, \omega) = i\pi[\delta(\omega - \omega_q) - \delta(\omega + \omega_q)]. \quad (4.12)$$

Taking into account that ω is of the order of T and much smaller than qv_F , we can put $\omega = 0$ in the function $\Phi(q, \omega)$ (Eq. 2.5). After integrating over ω , Eq. 2.1 takes the form

$$\frac{\delta_{e-ph}\sigma}{\sigma_3} = -2\tau^2 \int \frac{q^2 dq}{2\pi^2} f(\omega_q) \Re\Phi(q), \quad (4.13)$$

where $\Phi(q) = \Phi(q, \omega = 0)$.

In metals, $\Re\Phi(q)$ is calculated with the electron-phonon vertex γ_{met} in the static limit (Eq. 4.7). From Eq. 2.5, we get

$$\Re\Phi(q) = \left(\frac{16}{\pi^2} - 1 \right) \left(\frac{\pi}{2ql} \right)^2 \left(\frac{2}{3}\epsilon_F \right)^2 \frac{q^2}{2\rho\omega_q}. \quad (4.14)$$

Substituting this result into Eq. 4.13, we find

$$\frac{\delta_{e-ph}^{met}\sigma}{\sigma_3} = \left(1 - \frac{\pi^2}{16}\right) \frac{2\pi^2\beta_l T^2}{\epsilon_F p_F u_l}, \quad (4.15)$$

where the electron-phonon interaction constant is

$$\beta_l = \left(\frac{2}{3}\epsilon_F\right)^2 \frac{\nu}{2\rho u_l^2}. \quad (4.16)$$

Note, that in the isotropic model the deformation potential for transverse phonons is $-(3/2)G\sin(2\theta)$. Taking into account the interaction with transverse phonons, we will get Eq. 1.1 obtained in the paper².

For a bulk semiconductor, Eq. 2.5 with the vertex γ_{sem} (Eq. 4.5) results in

$$\Re\Phi(q) = -\left(\frac{\pi}{2ql}\right)^2 \left(\frac{q^2}{q^2 + \kappa_3^2}\right)^2 \frac{D_0^2 q^2}{2\rho\omega_q}. \quad (4.17)$$

At low temperatures, $T < \kappa_3 u$, the deformation potential is strongly screened. In this limit, the interference correction to the conductivity is given by

$$\frac{\delta_{e-ph}^{sem}\sigma}{\sigma_3} = -\frac{10\pi^6}{63} \frac{D_0^2 T^6}{\rho v_F^2 u^7 \kappa_3^4}. \quad (4.18)$$

At higher temperatures, $T > \kappa_3 u$, the deformation potential is not screened. In this limit Eqs. 4.13 and 4.17 result in

$$\frac{\delta_{e-ph}^{sem}\sigma}{\sigma_3} = -\frac{\pi^2}{24} \frac{D_0^2 T^2}{\rho v_F^2 u^3}. \quad (4.19)$$

For a two-dimensional electron gas in heterostructures interacting with three-dimensional phonons, Eq. 2.5 takes the form

$$\Re\Phi(q) = -\frac{2}{(q_{\parallel}l)^2} \left(\frac{q_{\parallel}}{q_{\parallel} + \kappa_2}\right)^2 \frac{D_0^2 q^2}{2\rho\omega_q}, \quad (4.20)$$

where q_{\parallel} is the wavevector component along the conducting plane, $\kappa_2 = 2\pi e^2 \nu_2$, $\nu_2 = m/\pi$.

Therefore, at low temperatures, $T < \kappa_2 u$, the correction to conductivity is given by

$$\frac{\delta_{e-ph}^{sem}\sigma}{\sigma_2} = -\frac{2\pi^2 D_0^2}{5\rho v_F^2 u^5 \kappa_2^2} T^4, \quad (4.21)$$

and, in the opposite limit,

$$\frac{\delta_{e-ph}^{sem}\sigma}{\sigma_2} = -\frac{D_0^2}{3\rho v_F^2 u^3} T^2 \ln \frac{T}{T_1}, \quad (4.22)$$

where $T_1 = \max\{u\kappa_2, u/l\}$.

In semiconductors the constant D_0 is much larger than G , therefore, in isotropic semiconductors interaction with longitudinal phonons plays a key role. The interference correction to conductivity is negative (Eqs. 4.18, 4.19,

TABLE II: Corrections to the conductivity $\delta_{e-ph}\sigma/\sigma_n$ due to the interaction of electrons with thermal phonons through the deformation potential.

	D=3	D=2
$T < \kappa_n u$	$-\frac{10\pi^6}{63} \frac{D_0^2 T^6}{\rho v_F^2 u^7 \kappa_3^4}$	$-\frac{2\pi^2 D_0^2}{5\rho v_F^2 u^5 \kappa_2^2} T^4$
$T > \kappa_n u$	$-\frac{\pi^2}{24} \frac{D_0^2 T^2}{\rho v_F^2 u^3}$	$-\frac{D_0^2}{3\rho v_F^2 u^3} T^2 \ln \frac{T}{T_1}$

κ_n is the inverse screening length, D_0 is the deformation potential, u is the sound velocity, and ρ is the density.

4.21, and 4.22) and results in the resistivity increases with temperature.

Results obtained in this section have simple physical interpretation. In the limit of weak disorder, $ql > 1$, the interference can be described by effective large-angle electron scattering process with square of the matrix element $a_{e-ph}^2/(ql)$, where a_{e-ph} is the matrix element of the 'pure' electron-phonon scattering. Therefore, in the Bloch-Gruneisen regime, the interference contribution to the conductivity turns out to be $(p_F/q)^2/(ql)$ times larger than the contribution of pure electron-phonon scattering. In the case of the Debye phonon spectrum, the corresponding temperature dependence of conductivity is modified by T^{-3} factor.

As it follows from the interpretation above, the interference corrections due to the electron-phonon interaction critically depend on the dimension of phonons and phonon spectrum. For example, flexural modes with dispersion $\omega_q \propto q^2$ dominate in the electron scattering in free standing thin films at low temperatures. In the Bloch-Gruneisen regime, the conductivity of pure films¹⁸ is proportional to $T^{7/2}$, then in weakly disordered films this dependence is proportional to T^2 .

V. CONCLUSIONS

In this work we investigated the interference of electron-electron (electron-phonon) scattering and elastic electron scattering from impurities and defects in weakly disordered conductors and heterostructures. We have calculated the interference corrections to the conductivity and demonstrated that even weak disorder significantly modifies its temperature dependence.

In weakly disordered conductors, characteristic momentum transfers are of the order of T/v_F , which is significantly smaller than the Fermi momentum. Therefore, the Landau Fermi-liquid theory is applicable and all processes with the large momentum transfer are taken into account by the effective Fermi-liquid constants. Both singlet and triplet channels of the electron-electron in-

teraction give interference corrections to conductivity,

$$\delta_{ee}\sigma = \delta_{ee}^s\sigma + \delta_{ee}^t\sigma. \quad (5.1)$$

Due to the Coulomb potential divergence at small momenta, the singlet-channel interaction corresponds to the unitary limit and corresponding corrections are independent on the Fermi-liquid parameters (see Tab. 1). The triplet-channel corrections (Eqs. 3.39 and 3.41) have the same temperature dependence as the singlet-channel corrections. Contrary to the singlet channel, the triplet channel corrections are not universal. Therefore, the value and sign of the total correction depend on the Fermi-liquid parameter F_0^σ in the triplet channel. In the weak coupling limit, $|F_0^\sigma| \ll 1$, the singlet-channel dominates over the triplet one and the corrections to conductivity are positive. Negative values of F_0^σ may result in the negative total correction, which is observed in heterostructures.¹⁴

Our main results for the singlet channel are summarized in Tab. I. We found that in weakly disordered bulk conductors the electron-electron interaction results in $T^2 \ln T$ - term in conductivity (Eq. 3.14). In a quasi-two-dimensional conductor, $d < v_F/T$, with 3D electron spectrum, $p_F d \gg 1$, the electron-electron interaction results in T -term (Eq. 3.22), which is the leading temperature-dependent term at subkelvin temperatures. Our result differs from that for 2D electrons¹¹ by a numerical factor. In the quasi-ballistic case, integrals of electron Green functions for quasi-two-dimensional conductors with 3D and 2D spectra (Eqs. 3.18 and 3.35) are significantly different and result in different coefficients.

In quasi-one-dimensional conductors with 3D and 2D spectra (wires and channels), the interference corrections are proportional to $\ln(T)$ (Eqs. 3.29 and 3.37). Note, that at sub-Kelvin temperatures the characteristic length, $d_c = v_F/T$, is of the order of 1 - 10 μm . Therefore, experiments with wires and channels of μm -sizes would allow to observe crossovers to lower dimensions. Note, that the logarithmic term has been recently observed in arrays of open quantum dots of μm -sizes at sub-Kelvin temperatures.¹⁹ This observation may be relevant to the quasi-one-dimensional interference corrections calculated in this paper.

We considered the electron-electron interaction via virtual phonons and found that this interaction results in

$T^2 \ln T$ -term (Eq. 4.9). The interference corrections due to interaction of electrons with thermal phonons are summarized in Tab. II. In bulk semiconductors at low temperatures, $T < \kappa_3 u$, the contribution of thermal phonons interacting with electrons via the screened deformation potential results in T^6 -term (Eq. 4.18). At higher temperatures the interaction via unscreened deformation potential results in T^2 -term (Eq. 4.19). In two-dimensional heterostructures the screened deformation potential leads to T^4 -term (Eq. 4.21) and the unscreened deformation potential results in $T^2 \ln T$ -term (Eq. 4.18).

The effects of the electron-electron interaction dominate in conductivity of weakly disordered conductors at low temperatures. At higher temperatures, conductivity is determined by the electron-phonon-impurity interference and then the pure electron-phonon scattering prevails over the interference mechanisms. Relative values of interference terms and characteristic crossover temperatures depend on many parameters. The effects of the electron-electron interaction are enhanced in low-dimensional conductors. As we discussed in Sec. IV, at low temperatures the contribution of the electron-phonon-impurity interference turns out to be $(p_F/q_T)^2/(q_T l)$ times larger than the contribution of pure electron-phonon scattering. Therefore, the interference contributions dominate over pure electron-phonon scattering at $T \leq up_F(p_F l)^{-1/3}$. It is important, that all interference corrections are proportional to the Drude conductivity, and this characteristic feature may be used for their experimental identification, as it has been done for metallic films.³

Note, that the T^2 -term has been actually widely observed in conductivity of doped semiconductors. It was associated with strongly anisotropic Fermi surfaces and electron-electron scattering (for a review see the book¹⁷). In our opinion, the electron-phonon-impurity interference correction is a more plausible reason for such term.

Acknowledgments

The research was supported by the ONR grant. We would like to thank I. Aleiner, J. Bird, M. Gershenson, B. Narozhny, and D. Maslov for useful discussions.

* Electronic address: sergeev@ciao.eng.wayne.edu

¹ B. L. Altshuler and A. G. Aronov, *Electron-Electron Interaction in Disordered Systems*, edited by A. L. Efros and M. Polak (North-Holland, Amsterdam, 1985).

² M. Yu. Reizer and A. V. Sergeev, Zh. Eksp. Teor. Fiz. **92**, 2291 (1987) [Sov. Phys. JETP **65**, 1291 (1987)].

³ N.G. Ptitsina, G.M. Chulkova, K.S. Il'in et. al, Phys. Rev. B **56** 10089 (1997).

⁴ K.S. Il'in, N.G. Ptitsina, A.V. Sergeev et. al, Phys. Rev. B

57, 15623 (1998).

⁵ A. Sergeev, B.S. Karasik, N.G. Ptitsina et. al, Physica B **263-264**, 190 (1999).

⁶ A. Stolovits, A. Sherman, T. Avarmaa, O. Meier, and M. Sisti, Phys. Rev. B **58**, 11111 (1998).

⁷ M. Reizer, Phys. Rev. B **57**, 12338 (1998).

⁸ A. Gold and V.T. Dolgoplov, Phys. Rev. B **33** 1076 (1986).

⁹ F. Stern and S. Das Sarma, Solid State Electron. **28** 158

- (1985).
- ¹⁰ D.V. Khveshchenko and M. Reizer, cond-mat/9609174.
- ¹¹ G. Zala, B.N. Narozhny, and I.L. Aleiner, Phys. Rev. B **64**, 214204 (2001).
- ¹² Y.Y. Proskuryakov, A.K. Savchenko, S.S. Safonov et al., Phys. Rev. Lett. **89**, 076406 (2002).
- ¹³ H. Noh, M.P. Lilly, D.C. Tsui, J.A. Simmons, E.H. Hwang, S. Das Sarma, L.N. Pfeifer, and K.W. West, cond-mat/0206519.
- ¹⁴ V.M. Pudalov, E.M. Gershenson, A. Kojima, G. Brunthaler, A. Prinz, and Bauer, cond-mat/0205449.
- ¹⁵ S.A. Vitkalov, K. James, B.N. Narozhny, M.P. Sarachik, and T.M. Klapwijk, cond-mat/0204566.
- ¹⁶ S. Koshino, Prog. Theor. Phys, **24**, 484 (1960), P.L. Taylor, Phys. Rev. A **135**, 1333 (1964), Yu. Kagan and A.P. Zhernov, Zh. Eksp. Teor. Fiz. **50**, 1107 (1966) [Sov. Phys. JETP **23**, 737 (1967)].
- ¹⁷ V.F. Gantmakher and Y.B. Levinson, *Carrier Scattering in Metals and Semiconductors*, North-Holland, Amsterdam, Oxford, New York, Tokyo (1987).
- ¹⁸ B.A. Glavin, V.I. Pipa, V.V. Mitin, and M.A. Stroschio, Phys. Rev. B **65** 205315 (2002).
- ¹⁹ A. Shailos, J.P. Bird, C. Prasad et al, Phys. Rev. B **63** 241302(R) (2001).
- ²⁰ A.I. Larkin and Yu.N. Ovchinnikov, Zh. Exsp. Teor. Fiz. **55**, 2262 (1968) [Sov. Phys. JETP **28**, 1200 (1969)].
- ²¹ M. Reizer, A. Sergeev, J.W. Wilkins, and D. Livanov, Annals of Phys. **257**, 44 (1997).

APPENDIX: QUANTUM TRANSPORT EQUATION

The goal of this section is to show how the basic equations discussed in Sec. II are obtained in the formalism of the quantum transport equation. This method is based on the Keldysh diagrammatic technique, where the electric current is expressed through the kinetic (Keldysh) component of electron Green function, $G^C(\mathbf{p}, \epsilon)$, in the following way

$$\mathbf{J}_e = \sigma \mathbf{E} = e \int \frac{d\mathbf{p}d\epsilon}{(2\pi)^4} \mathbf{v} \text{Im}G^C(\mathbf{p}, \epsilon). \quad (\text{A.1})$$

Without interaction effects, the expressions for electron Green functions in disordered conductors are well known. The retarded (R) and advanced (A) electron Green functions are

$$G_0^R(\mathbf{p}, \epsilon) = [G_0^A(\mathbf{p}, \epsilon)]^* = (\epsilon - \xi_p + i/2\tau)^{-1}, \quad (\text{A.2})$$

and $\xi_p = (p^2 - p_F^2)/2m$. The kinetic component of the electron Green function is given by

$$G_0^C(\mathbf{p}, \epsilon) = 2i S(\mathbf{p}, \epsilon) \Im[G_0^A(\mathbf{p}, \epsilon)] + \delta G_0^C, \quad (\text{A.3})$$

$$\delta G_0^C = \frac{1}{2} \{S_0(\epsilon), G_0^A + G_0^R\}. \quad (\text{A.4})$$

where the electron distribution function is given by

$$S(\mathbf{p}, \epsilon) = S_0(\epsilon) + \phi(\mathbf{p}, \epsilon), \quad (\text{A.5})$$

$$S_0(\epsilon) = -\tanh(\epsilon/2T), \quad (\text{A.6})$$

$$\phi(\mathbf{p}, \epsilon) = -e\tau(\mathbf{v} \cdot \mathbf{E}) \frac{\partial S_0(\epsilon)}{\partial \epsilon}. \quad (\text{A.7})$$

The nonlocal correction $\delta G_0^C(\mathbf{p}, \epsilon)$ has a form of the Poisson bracket,

$$\{A, B\} = e\mathbf{E} \left(\frac{\partial A}{\partial \epsilon} \frac{\partial B}{\partial \mathbf{p}} - \frac{\partial B}{\partial \epsilon} \frac{\partial A}{\partial \mathbf{p}} \right). \quad (\text{A.8})$$

The kinetic Green function G_0^C (Eq. A.3) with the distribution function $S(\mathbf{p}, \epsilon)$ (Eq. A.5) takes into account only elastic electron scattering from impurities. Substituting G_0^C in Eq. A.1, one could get the Drude conductivity. The nonlocal correction $\delta G_0^C(\mathbf{p}, \epsilon)$ is required to satisfy the unitary condition for the matrix Keldysh function,²⁰ it removes divergence in Eq. A.1 far from the Fermi surface.

Assuming that the elastic electron scattering from impurities and defects dominates in the electron momentum relaxation, one can apply the iteration procedure to the Dyson equation. Then the many-body correction to the kinetic Green function is expressed through the electron self-energy in the following way²¹,

$$\begin{aligned} \delta_{int}G^C &= 2\tau [\Sigma_{int}^C - 2i S \Im \Sigma_{int}^A] \Im G_0^A \\ &+ 2\tau \{ \Re \Sigma_{int}^A, S_0 \} \Im G_0^A + S \Im \Sigma_{int}^A (G_0^A)^2. \end{aligned} \quad (\text{A.9})$$

Note, that the electric field enters Eq. A.9 through the nonequilibrium distribution function $\phi(\mathbf{p}, \epsilon)$ (Eq. A.5) and the electric Poisson bracket (Eq. A.8), the interaction is included in components of the electron self-energy.

For weakly disordered conductor we should consider three electron self-energy diagrams shown in Fig. 1. The first diagram does not consists of dotted lines corresponding to the electron-impurity interaction. Electron-impurity scattering is included only in the electron Green functions (Eq. A.2). Therefore, without nonlocal quantum corrections in the form of the Poisson brackets (Eq. A.8), the first diagram results in the Bloch-Gruneisen term. Interference effects are taken into account by the Poisson bracket terms. Namely, δC_0^C (Eq. A.3) has to be taken into consideration in all self-energy components (A,R,C) in the first term in Eq. A.9. The second term has the Poisson bracket form and, therefore, it is directly calculated with the equilibrium distribution functions. Substituting $\delta_{int}C^C$ in Eq. A.1, we get the correction to the conductivity in the form of Eqs. 2.1 and 2.3 with the function $\Phi(q, \omega)$ given by

$$\begin{aligned} \Phi_1(q, \omega) &= \frac{i n}{4\pi l^2} \int d\xi_p \langle \langle \gamma^2(\mathbf{v} \cdot \mathbf{e})^2 [G^R(\mathbf{q} + \mathbf{p}, \epsilon + \omega)]^2 \\ &\times G^A(\mathbf{p}, \epsilon) \rangle \rangle_{\mathbf{v}, \mathbf{q}} = -\frac{1}{2\tau^2 v_F^2} \left\langle \left\langle \frac{\gamma^2(\mathbf{v}_F \cdot \mathbf{e})^2}{(\mathbf{q}\mathbf{v}_F - \omega - i0)^2} \right\rangle \right\rangle_{\mathbf{v}, \mathbf{q}}. \end{aligned} \quad (\text{A.10})$$

In the second and third diagrams the electron-impurity and electron-electron (electron-phonon) interactions are directly presented. Therefore, interference contributions of these diagrams originate from the first term in Eq. A.9 without any Poisson bracket corrections. Calculations show that the contribution of the second diagram

is exactly the same as the first one,

$$\Phi_2(q, \omega) = \Phi_1(q, \omega). \quad (\text{A.11})$$

The third diagram with the vertex γ renormalized by elastic electron-impurity scattering gives

$$\Phi_3(q, \omega) = \langle K(q, \omega) \cdot L(\mathbf{q}, \omega) \rangle_{\mathbf{q}} - \langle [M(\mathbf{q}, \omega)]^2 \rangle_{\mathbf{q}}. \quad (\text{A.12})$$

The first term in Eq. A.12 corresponds to the third diagram with the equilibrium vertex, which is given by

$$\begin{aligned} K(q, \omega) &= \frac{1}{\pi\nu_n\tau} \int \frac{d\mathbf{p}}{(2\pi)^n} \gamma G^A(\mathbf{p}, \epsilon) G^R(\mathbf{p} + \mathbf{q}, \epsilon + \omega) \\ &= -\frac{i}{\tau} \left\langle \frac{\gamma}{\mathbf{q}\mathbf{v}_F - \omega - i0} \right\rangle_{\mathbf{v}}, \end{aligned} \quad (\text{A.13})$$

and the rest of the diagram is described by the function

$$\begin{aligned} L(\mathbf{q}, \omega) &= \frac{1}{\pi\nu_n\tau} \int \frac{d\mathbf{p}}{(2\pi)^n} G^A(\mathbf{p}, \epsilon) G^R(\mathbf{p} + \mathbf{q}, \epsilon + \omega) \\ \times \frac{\gamma(\mathbf{v} \cdot \mathbf{e})^2}{v^2} &= -\frac{i}{\tau v_F^2} \left\langle \frac{\gamma(\mathbf{v}_F \cdot \mathbf{e})^2}{\mathbf{q}\mathbf{v}_F - \omega - i0} \right\rangle_{\mathbf{v}}. \end{aligned} \quad (\text{A.14})$$

The nonequilibrium vertex calculated with the distribution function $\phi(\mathbf{p}, \epsilon)$ leads to

$$\begin{aligned} M(\mathbf{q}, \omega) &= \frac{1}{\pi\nu_n\tau} \int \frac{d\mathbf{p}}{(2\pi)^n} G^A(\mathbf{p}, \epsilon) G^R(\mathbf{p} + \mathbf{q}, \epsilon + \omega) \\ \times \frac{\gamma \mathbf{v} \cdot \mathbf{e}}{v} &= -\frac{i}{\tau v_F} \left\langle \frac{\gamma \mathbf{v}_F \cdot \mathbf{e}}{\mathbf{q}\mathbf{v}_F - \omega - i0} \right\rangle_{\mathbf{v}}. \end{aligned} \quad (\text{A.15})$$

Finally, summarizing $\Phi_i(q, \omega)$ (Eqs. A.10, A.11, and A.12), we get Eq. 2.4.

As we already mentioned, Eqs. 2.1 and 2.4 can be also derived in the linear response formalism.^{2,11} The corresponding diagrams are shown in Fig. 2. Here, the diagrams 1 and 2 corresponds to the first diagram of the transport equation method (Eq. A.10), the diagrams 3 corresponds to the second diagram (Eq. A.11), the diagrams 4 and 5 are equivalent to the third diagram with the equilibrium vertex (Eqs A.12 and A.13), and the diagrams 6 and 7 are equivalent to the third diagram with the nonequilibrium vertex (Eqs A.12 and A.15).

FIG. 1: Electron self-energy diagrams in the quasi-ballistic limit. Wavy line stands for to the electron-electron or electron-phonon scattering, a dotted line stands for to elastic electron scattering from random potential, and a straight line stands for the electron Green function.

FIG. 2: Diagrams of the conductivity in the linear response method.

FIG. 3: Screening of the electron-phonon vertex. The zigzag line stands for the Coulomb potential, $V(q, \omega)$.

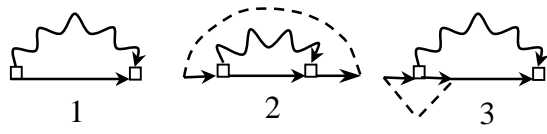


Fig. 1

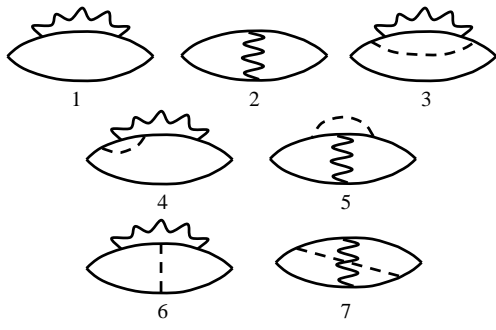


Fig. 2

The diagram shows an equation between three Feynman diagrams. The first diagram on the left consists of a wavy line with a vertex (a small circle) on it, with two external lines extending from the vertex. This is followed by an equals sign. To the right of the equals sign are two terms added together. The first term is identical to the first diagram. The second term is a wavy line with a vertex, where the vertex is connected to a loop (a circle) that also has a wavy line segment, which then connects back to the vertex. This loop structure is attached to the vertex of the wavy line.

Fig. 3